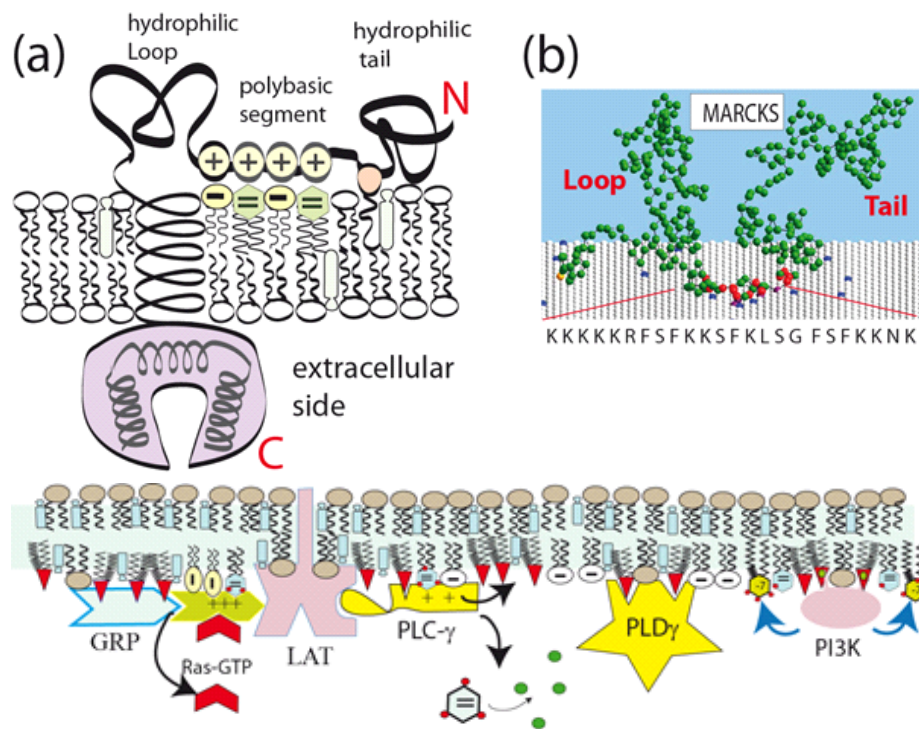


Supplements and Updates to Kapitel 9

Complementary Chapter to Sackmann/Merkel 'Lehrbuch der Biophysik'



Copyright Erich Sackmann, Physics Department Technical University Munich.

The text can be freely downloaded via the website www.biophy.de.

9.A.1 Hydrophobic-electrostatic membrane coupling of proteins

Introduction

In Chapter 9-13 we introduced the basic physical principles of the self organization and function of cell membranes, with major emphasis on the control of the molecular organization by selective lipid-protein interaction (c.f. also [Sackmann 1996]). In the chapters 18-28 on the physics of cells it became evident that biological membranes are composite shells the structure and function of which is determined by the interplay of the lipid-protein bilayer and the membrane associated scaffold. A prototype of the composite cell membrane is the erythrocyte envelope. The intimate crosstalk between the two subshells implies that any structural change in one leaflet evokes a conformational change in the other. However, the concept of the composite biomembrane is more general. It also comprises the lipid protein bilayer with dynamically coupled proteins which play a key role for the formation of functional domains such as immunological synapses (c.f. Chapter 39). The coupling of extrinsic proteins and to membranes can be mediated by several mechanisms:

1. By specific interaction between the cytoplasmic domains of integral proteins and actin membrane linkers
2. By direct coupling to the lipid bilayer through the combination of electrostatic and hydrophobic forces
3. By salt bridges mediating the coupling between basic amino acids of the protein and negatively charged lipids such as phosphatidylserine and phosphoinositides.

Prominent examples of the first mechanism are proteins exposing the FERM homology domains (such as Band IV.1 and talin) which couple actin to cytoplasmic tails of integral cell adhesion

molecules (such as integrins, cadherins and band IV.1, c.f. Ch.13). The second mechanism is discussed extensively below. The most prominent examples of the Ca-mediated binding are the annexins (s. Ch. 9 and [Gerke 2002]).

This supplemental chapter deals with the physics of biological membrane processes mediated by transient coupling of extrinsic proteins to the inner leaflet of plasma membranes or the outer leaflet of intracellular organelles, with major emphasize on the hydrophobic-electrostatic mechanism of protein-to-membrane linkage. We start with the discussion of the protein absorption by electrostatic-hydrophobic interaction of proteins with polybasic sequences to membranes containing phosphatidylserine and phosphoinositides (PIP2, PIP3). We then show various mechanisms of protein adsorption by specific interaction of specific homology domains with lipids. These lipids can thus function as second messenger which transmits external cues into intracellular signaling and can couple signaling pathways initiated by different enzymes. An outstanding example is the stimulation of lymphocytes by transient encounters with antigen presenting cells presented in Chapter 39. Numerous keywords are defined in the Glossary to this Chapter.

The hydrophobic electrostatic interaction plays a key role for the recruitment and activation of GTPases, such as Ga fractions of heterogeneous $G_{\alpha\beta\gamma}$ -molecular switches (see Kapitel 9) as well as the small GTPases of the Ras superfamily. To set the stage let us consider a member of the Ras-subfamily. In the resting state of the cells the small GTPases reside in the cytoplasm in a sleeping configuration which is stabilized by the binding of guanosine- nucleotide dissociation inhibitors (GDIs see Glossary to Chapter 39). They are activated by binding of guanine exchange factors (GEF) which displaces the inhibitor and results in their recruitment to the plasma membrane (see Ch.S.9.1). They couple to the membrane via hydrophobic chains, electrostatic forces, or both (see Figs S.9.1 and 9.2). A classic example is the GTPase $p21^{ras}$ which is involved in the stimulation of the ERK-MAPK pathway of lymphocytes described in Chapter 39 (see [Hancock 1990]). The protein family comprises three members: H, K,

und N and are composed of a conserved region and a hypervariable segment (see Fig S.9.1). The former determines the biochemical functions, while the latter control the coupling to the membranes and other proteins.

A common feature of all three members (H, K, N) is that the segment -AAX at the C-terminal undergoes a posttranslational modification at the C-terminal. The -AAX- domain is cleaved off (by a protease) and a poly-isoprenoid group is coupled to the Cysteine (C). The second modification differs for the three members. The N-Ras is modified by coupling of a single palmitic acid chain to the amino acid 181 while the H-Ras binds via two palmitoyl groups. In contrast the K-Ras exhibits only a polybasic domain composed of 6 consecutive lysine groups.

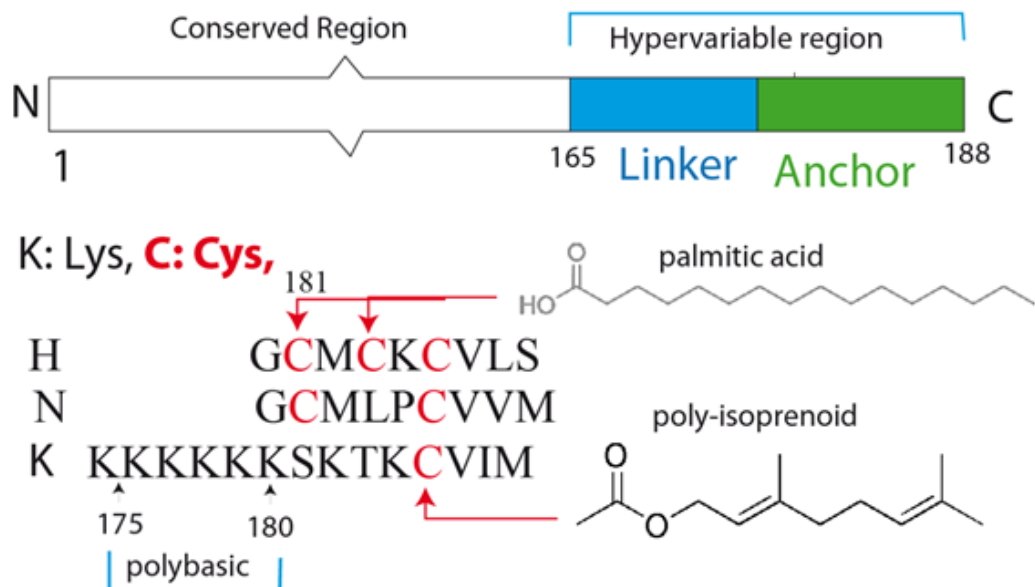


Fig. S.9.1: Schematic view of the structure of the Ras-proteins $p21^{Ras}$ (H, K, N). They consist of the hypervariable domain at the C-terminal (amino acids 165-189) and the conserved segment 1-164 at the N-terminal. To generate the functional proteins the proteins are modified in two ways as described in the text.

Numerous studies showed that the Ras proteins are only functionalized by recruitment to the

plasma membrane if they contain either a palmitoyl chains or the polybasic sequence. If the lysine groups are replaced by acidic amino acids they unbind from the membrane if more than four lysines are replaced ([Hancock 1990]). Remarkably, it has been observed that the replacement of the palmitoyl group by myristic acid (a chain with C14 C-atoms) abolishes membrane binding, and thus the function of Ras, unless they exhibit polybasic sequences. Palmitoyl chains appear to be absolutely required for the activation of Ras proteins by membrane binding. These observations suggests that the electrostatic and hydrophobic forces are adjusted in such a way that the GTPases can be easily displaced from the membrane by removal of a fatty acid or by phosphorylation the basic amino acids lysine and arginine, thus facilitating the exchange between the membrane and the cytoplasm. Some examples will be shown below.

MARCKS: A paradigm of electro-hydrophobic membrane association of proteins

The MARCKS protein (myristoylated alanine-rich C-kinase substrate) is an intensively studied example of hydrophobic-electrostatic membrane coupling of proteins (c.f. [Mc Laughlin 2002] and [Ben Shaul 2008]). The protein (332 amino acids) is composed of three sections. The N-terminal section (comprising the first $N_{loop} = 151$ segments) exposes a myristic acid chain at the end and forms a loop anchored at both ends. The central part consists of a polybasic section comprising 12 lysine and one arginine group which are interrupted by short sections of neutral and polar amino acids, including four polar serine and five hydrophobic phenylalanines. The C-terminal comprising segment 177-332 ($N_{tail} = 155$) is composed of a mixture of all types of amino acids (including five acidic peptides). The serines can act as electrostatic enabling the unbinding of MARCKS by phosphorylation [Mc Laughlin 2002]. The most probable structure of the membrane bound MARCKS (as suggested by Monte Carlo studies) is shown in Fig S. 9. 2.

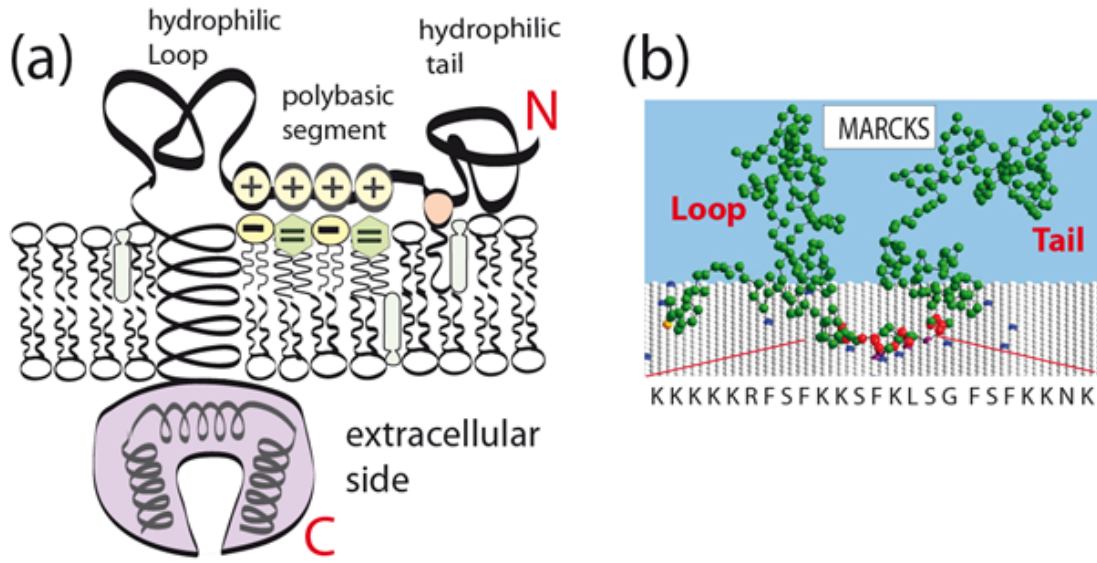


Fig. S.9.2: Left: Model of integral membrane proteins, simultaneously interacting with lipid bilayers by electrostatic and hydrophobic forces. Examples are the transferrin receptor (Kapitel 9) and LAT (see Chapter 39). Right: Birds view of MARCKS protein anchored in membranes by myristic acid located at the C-terminal. The basic section comprises 13 amino acids (with K≡ Lysine; R≡ arginine; S≡serine; F≡phenylalanine; G≡ glycine; L≡leucine). The N-tail and the loop between the fatty acid anchor and the first basic amino acid extend into the aqueous phase. The protein plays a manifold of roles which are not understood yet.

The free energy difference between the free and the membrane bound MARCKS has been evaluated by Monte Carlo (MC) studies [Ben Shaul 2008]. The method provides semi-quantitative but valuable insights into the balance between the enthalpic and entropic contribution to the work of protein adsorption. The total free binding energy difference between the free and bound state (called the adsorption free energy) is determined by four contributions:

$$\Delta F_{tot} = \Delta F_{pbs} + \Delta F_{loop} + \Delta F_{tail} + \Delta F_B + \Delta F_c$$

(S.9.1)

ΔF_{pbs} accounts for the free adsorption energy of the polybasic sequence (where pbs stands for polybasic basic sequence), ΔF_B is the Born self-energy, ΔF_{loop} and ΔF_{tail} are the free energies of the loop and the tail with $\Delta F_i = \Delta U_i - T\Delta S_i$ (where i stands for loop or tail) and ΔF_c is the energy gain associated with the penetration of the fatty acid anchors into the lipid monolayer. In the following we discuss first the physical basis of the above contributions to the free adsorption energies. Numerical results are summarized in Table I, followed by a summary of the major results and a critical assessment of the model.

1. Consider first the free adsorption energy of the polybasic sequence (ΔF_{pbs}). It consists of two contributions: the electrostatic interaction between the charged amino acids and lipids (ΔF_{el}) and the energy (ΔF_{hph}) gain due to the penetration of the hydrophobic amino acids (in particular phenylalanine) into the semipolar region of the lipid bilayer:

(ΔF_{el}) is calculated on the basis of a modified Debye-Hückel theory which accounts for the fact that the pair interaction potential between two charges q and q' is modified near the membrane surface, due to the large difference between the dielectric constants of water ($\epsilon \approx 80$) and the lipid layer ($\epsilon \approx 2.5$). Following R. Netz [Netz 1999], ΔF_{el} can be expressed as:

$$\Delta E_{el} = qq'l_B \frac{\exp\{-\kappa r\}}{r} + qq'l_B \frac{\exp\{-\kappa \sqrt{r^2 + 4zz'}\}}{\sqrt{r^2 + 4zz'}}$$

(S.9.2)

Where r is the distance between the point charges q , q' and z , z' are the distances from the interface. l_B is the Bjerrum length (introduced in Ch.24.8) and for our situation it is $l_B \approx 0.72$ nm. κ^{-1} is the Debye screening length. For physiological intracellular ion strengths (~ 0.2 M) it is about 0.6-0.7nm. Since z and z' are similar to the ion distance r the interfacial correction term is of the same order of magnitude as the pair potential. The two contributions are equal if $z = z' \approx 0$.

The hydrophobic side chains of the neutral amino acids within the polybasic segment are assumed to penetrate into the hydrophobic region of the membrane and to contribute to the binding energy. This is suggested by the observation that hydrophobic amino acids bind remarkably strongly to lipid bilayers [Whimley 1996]. From the partition coefficients of amino acids between water and membranes, binding energies of $-1 k_B T$ (for alanine) and $-6 k_B T$ (for phenylalanine) have been estimated. The MC simulation yields an electrostatic binding energy of $\Delta F_{pbs} = -42 k_B T$. Due to the strong adsorption the conformational freedom is strongly reduced as demonstrated by the large entropic energy costs of $30 k_B T$ reducing the free adsorption energy to $\Delta F_{pbs} = -12.5 k_B T$.

2. Consider next the contributions of the loop and the tail ($\Delta E_{loop}, \Delta F_{tail}$). The enthalpic contribution is determined by the excluded volume interaction of the surface grafted segments. It is calculated by accounting for the steric repulsion between the segments in terms of Lennard Jones potentials. The entropic contribution is determined by the reduction in conformational degrees of freedom by fixing the chains on the surface. For the tail domain (fixed at one end), ΔS_{tail} can be estimated by the following approximation equation:

$$\Delta S_{tail} = k_B T \ln N^{1/2}$$

(S.9.3)

yielding $k_B T \Delta S_{tail} \sim 2.5 k_B T$ for $N_{tail} = 155$, in excellent agreement with the value obtained by the MC-simulation. The value for the loop domain is by a factor of three larger ($k_B T \approx 7.5 k_B T$).

3. The membrane water interface modifies also the Born self-energy which accounts for the energy costs associated with the charging of the ions at a distance z from the membrane surface.

Following [Netz 1999] it can be expressed as

$$\Delta E_{Born} = \frac{q^2}{2} l_B \frac{\exp\{-2\kappa z\}}{2z}$$

The total contribution is small $\Delta E_{Born} \sim 0.8k_B T$.

4. Finally we consider the hydrophobic binding energy gain (ΔF_c) of the Lipid anchors. It can be estimated by the following empirical rule law suggested by measurements of the critical micelle (or vesicle formation) concentrations [Sackmann1995]

$$\Delta G_c = (11 - 3n) kJ M^{-1}$$

(S.9.4)

where n is the number of CH_2 groups. For myristic acid: $\Delta G \sim 31 \frac{kJ}{M} (\approx 13k_B T)$ and for palmitic acid: $\approx 15k_B T$.

Table I shows some pertinent numerical results for membranes composed of 89

In the following some remarkable predictions of the MC-simulation are summarized which are considered to be helpful to readers interested in the quantitative evaluation of the membrane binding strengths of proteins exhibiting polybasic sequences.

Balance of hydrophobic and electrostatic binding

Contribution	ΔF_{pbs}	$T \Delta S_{pbs}$	$\Delta F_{tail} + \Delta F_{loop}$	ΔF_C	ΔF_{tot}
Wild Type*	-42	+ 30	+12.5	-15.2	-15
Mutant*	-9	+18	+12.5	-12.5	+9

Table I: Pertinent data on contributions (defined in Eq.S.9.1) to free adsorption energy of MARCKS for physiological relevant lipid composition (89% PC), 10% PS 1% PIP2). Energies are given in units of $k_B T$. The second line shows the value for wild tape protein exposing 5 phenylalanines (F) in polybasic sequence. In the third column the contribution of the entropic energy costs caused by the membrane binding of the polybasic section to ΔF_{pbs} is given. The third line shows the values for the mutant in which all phenylalamines are replaced by the much smaller amino acid alanine.

Alanine (A)	Lysine (K)	Arginin (R)	Phenylalanine(F)	Tryptophan (W)
0.071	0.128	173	0.189	0.23

Table 2: Volumes of Amino acids in nm^3 . Data reproduced from Jena Library

Comparison of the entropic costs associated with the surface grafting of the loop and tail ($\Delta G_{tail} + \Delta G_{loop}$) and the gain (ΔG_c) due to the myristic acid shows that the two contributions nearly compensate each other (since $\Delta F_{tail} + \Delta F_{loop} + \Delta F_c \approx -2.5k_B T$). According to Eq.S4, with palmitic acid anchors one could increase the remaining binding energy gain by a factor of two (to $5.0k_B T$). Taken together, the above consideration shows that the protein binding strength can be controlled in a subtle way by balancing the electrostatic and hydrophobic forces. In particular, weak electrostatic forces can be overcompensated by protein coupling via two hydrophobic chains, such as in the case of H-Ras (see Fig S. 9.1).

A most remarkable result is revealed by comparing the data for 9:1 PC: PC mixtures in the presence of absence of 1% PIP2. Addition of 1% PIP2 to 90:10 PC:PS mixed membranes increases the free adsorption energy of MARCKS by over a factor of two. The MC-simulation predicts that $n_{PIP2} \approx 4$ PIP2 lipids are attracted to the adsorbed protein. It should be noted, however, that the charge of PIP2 depends on the local pH and the interaction with protein [McLaughlin 2002]. At 1% PIP2 the first phosphate (at position 4 and 5 of the inositol group) dissociate at $pH \sim 6 - 7$ and the second at $pH \approx 7.7$. Thus at $pH > 7$ only one OH-group of the lipid is protonated resulting in a net charge of $q \approx -4$. On the other side, electrophoretic mobility measurements of vesicles (shown in Kapitel 11, Fig 11.13) yield a value of $q = 3$. Thus 4 bound PIP2 would be sufficient to compensate most of the 13 basic lipids.

However, the MC-simulations have to be considered with a grain of salt since it neglects two effects:

First one has to consider that the local pK-values of lipids at the surface of negatively charged membranes can be remarkably increased, due to proton repulsion by the membrane [reviews see [Sackmann 1995]] although the effect is small at physiological ionic strengths.

Secondly, the strong binding of PIP2 is most likely not only due to electrostatic forces but it is expected to be strengthened by hydrogen bonds. The key role played by hydrogen bonds for the specific binding of PIP2 to proteins, such as phospholipase C, is well established. In general the phosphoinositols PIP2 and PIP3 bind to the protein homology domain pleckstrin (see Fig S9.3b). As discussed in Kapitel 1 (Abbildung 1.5) strong H-bridges can only form if the two bonds mediating the H-bond are oriented parallel. Considering this constraint PIP2 one expects that two strong hydrogen bonds with the lysine groups could be formed (Fig. S. 9.3). The energy per H-bond of such bonds is $10 - 30 \frac{kJ}{M}$ or $8 - 12 k_B T$. This is certainly an upper limit since most potential H-bond forming ligands are saturated by H-bond with water.

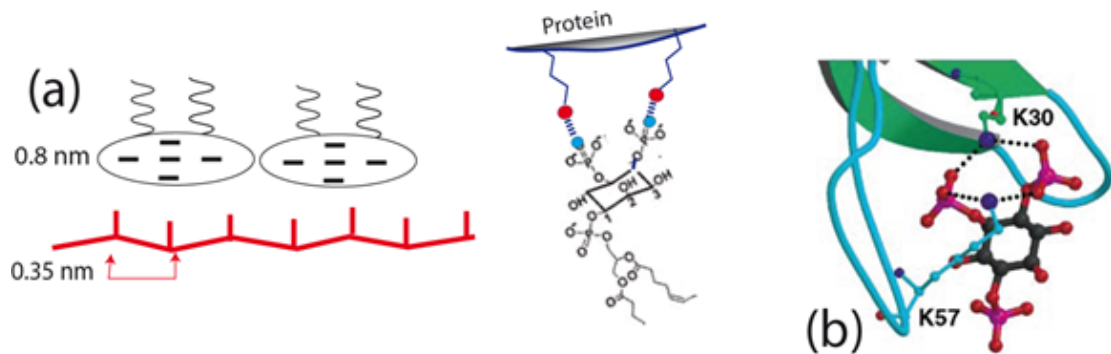


Fig. S.9.3. (a) Left: schematic view of distance of side chains of polybasic sequence and lateral dimension of lipid head group, showing that one PIP2 head group could interact with at least three basic amino acids. Right: schematic view of hydrogen bonds formed between lysine group of polybasic protein sequence and phosphates of PIP2 groups. b) Topological view of H-bond mediated binding of the PIP2 head group to the pleckstrin domain of phospholipase C which exhibits two lysine groups. Note that the hydrogen bond length is 0.18 nm.

Unbinding forces of hydrophobic anchors

The binding strength of lipid anchors can be measured by dynamic force spectroscopy techniques described in Kapitel 8.3, such as that shown in Fig. 8.23 and described in [Evans 1999]. In Kapitel 8.3 we showed that the rate of unbinding k_{off} depends on the force

(F) according to a modified Arrhenius equation (cf. Eq.8.2). It was shown that the force at which half of the molecules are unbound depends on the rate of force application $\frac{dF}{dt}$ according to:

$$F_{1/2} = F_o \left(1 + \frac{dF/dt}{k_o F_o} \ln 2 \right)$$

(S.9.5)

where F_o is the force amplitude and k_o is the off-rate at zero force. In Fig. S.9.4 distributions of unbinding forces for DSPE embedded in a fluid membrane of SOPC (stearoyl-oleyl-phosphatidylcholine) are shown for force rates of $50 \frac{pN}{sec}$ and $25 \cdot 10^3 \frac{pN}{sec}$, respectively. The average unbinding force increases from $F^* \approx 10$ to $F^* \approx 50 pN$. They are comparable to those between integrins and ICAM for which F^* raises from 25 pN at $100 \frac{pN}{sec}$ to 50 pN for $10^4 \frac{pN}{sec}$.

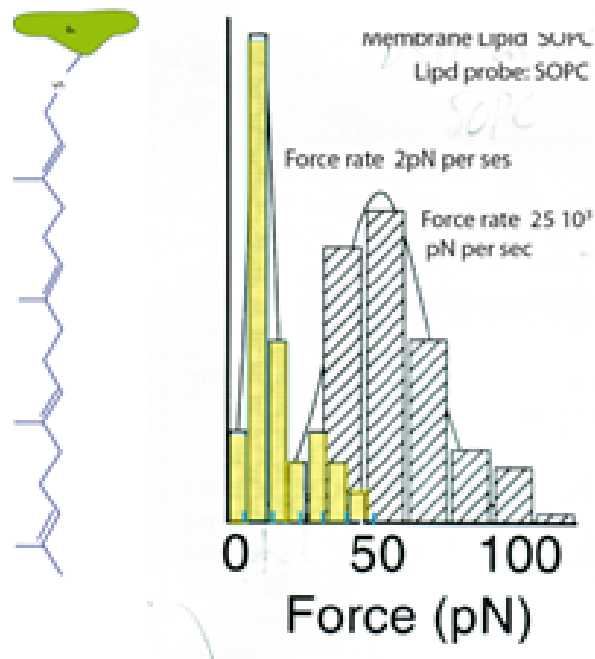


Fig. S.9.4: Right side: Distribution of unbinding forces of phospholipid (SOPS) from fluid membranes composed of SOPS measured by the micropipette technique (described in Kapitel 8.3). The force rates are indicated at the histograms. The left side shows the chemical structure of a geranygeranyl chain bound to a protein.

It is interesting and helpful to compare the work of lipid disruption from membranes, Δw , with the binding energies measured at equilibrium which can be estimated with Eq. S.9.4. Δw is of the order of $\Delta w \approx F * \delta$, where δ is the hydrophobic thickness of the lipid monolayer. Eq.(S.9.4) yields for SOPS: $\Delta w \approx 18k_B T$, while the unbinding force at 25nN yields, for $d \approx 2nm$ and $\frac{dF}{dt} \approx 25 \frac{pN}{sec}$, a value of $25k_B T$. The two methods yield comparable data on the binding strengths of lipid anchors showing that Eq. (S.9.4) yields reliable values of this parameter.

9.A.2 Electrohydrophobic switching of protein binding.

The activation of functional membrane proteins by electrohydrophobic switching of membrane binding is expected to play a key role for numerous cellular processes which require the rapid recycling of proteins between the cell envelope and the cytoplasm. Examples are the vesicle shuttling between the plasma membrane and the Golgi apparatus during endocytosis and exocytosis (see Fig. S.9.5) and the control of genetic expression by transcription factors activated via the MAPK-mediated pathway which will be discussed in a separate chapter (Chapter 39). In this section we will give a brief overview over some pertinent mechanism of protein-membrane coupling.

Switching of protein binding via phosphorylation

A well-studied example for this mechanism is the MARCKS protein. It can be phosphorylated at the 4 serine groups of the polybasic segment (by protein kinases C), resulting in strong electrostatic repulsion forces. The MC calculation predicts a reduction of the total free binding energy ΔF_{tot} from 15.0 to 5.3 $k_B T$ [BenShaul 2008]. As noted above, the hydrophobic binding energy mediated by the myristic acid chain is nearly compensated by the entropy cost due to the surface grafting of the hydrophilic chains. Therefore the binding strength is determined by the basic residues resulting in the detachment of the MARCKS protein after phosphorylation of the lysine and serine by protein kinase C, which is also often anchored to the membrane as will be discussed below [Vergeres 1995]. This mechanism of dynamic membrane coupling via the protein kinase C is also called myristoyl-electrostatic (or electrohydrophobic) switching.

Hydrophobic switching of protein binding

A more frequent and versatile switching mechanism is mediated through hydrophobic chains such as palmitic acid or geranylgeranyl chains. These lipid anchors are often attached (post-translationally) in the ER or Golgi. A unique feature of these anchors is that they can be

attached in a reversible way during cellular processes. Thus the palmitic acid chain is coupled to -CH group of cysteine chains by specific palmitoylation enzymes (forming a thiol-ester bond). Conversely the anchors can be and detached by protein-thioesterases. In a similar way, the geranylgeranyl anchors belong to the group of reversible hydrophobic anchors as shown in the following fundamental membrane process mediated by Rab-GTPases.

Rab-GTPases are members of the super family of Ras-GTPases [Wennerberg 2008]) which play a key role for the formation, processing and recycling of endocytotic vesicles (see summary [Rodman 2000]). Rab proteins induce the budding of vesicles from the plasma membrane, mediate the coupling to motor proteins involved in the transport between the plasma membrane and the intracellular compartments. They finally trigger the fusion with the appropriate target vesicle. Most importantly, at the end of the transport cycle, the costly Rab protein has to be recycled. This recycling is mediated by the guanine dissociation inhibitor (GDI) which unbinds the Rab GTPase from the membrane by decoupling of the two geranylgeranyl chains (see Fig S.9.3 and the summary [Rodman 2000]).

Before we explain Fig.S-9.3 the reader should be reminded of the fact that the Rab-GTPases are activated by the same universal mechanism as the Rac family members (see Glossary in Chapter 36). The protein is excited from a sleeping state with bound GDP into an activated conformation by $\text{GDP} \rightarrow \text{GTP}$ exchange. Frequently the resting state is further stabilized by binding of a guanine nucleotide dissociation inhibitor (GDI). The first step consists therefore in the displacement of the inhibitor by binding of the guanine exchange factors (GEF) which triggers the $\text{GDP} \rightarrow \text{GTP}$ exchange in a second step. Since the excited GTP-Raf are slowly hydrolysed, the deactivation is accelerated by binding of a third helper protein: the GTPase-activating proteins (abbreviated as GAP).

However, the Rab-proteins differ from the other members of the Ras superfamily in two important features. First, they are not coupled to membranes by polybasic sequences (as Rac or Ras)

but by hydrocarbon chains; mainly geranylgeranyl groups which are coupled to the C-terminal via amino acid sequences Cys-Ala-Cys-OCH₃ (or simply Cys-Cys-OCH₃). Secondly, whereas inactive (sleeping) members of the Ras family reside in the cytoplasm those of Rab-GTPases are bound to the membrane. The membrane linkage is mediated by the guanine nucleotide dissociation inhibitor (GDI) which is coupled to a membrane receptor [YuAn 2003]. Rab is activated by decoupling of the two lipid anchors from the membrane and the GTPase and their transfer to a binding pocket of the GDI. By this elegant mechanism the GPI can retrieve a large number of the 70 members of human Raf-GTPases.

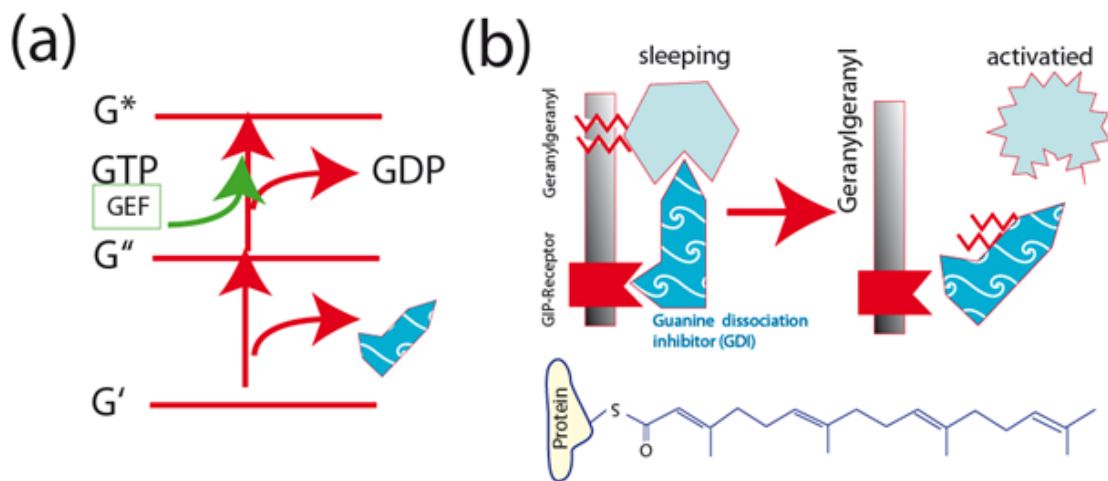


Fig. S.9.5:(a) Schematic view of activation of sleeping GTPases in two steps: the unbinding of the inhibitor and the replacement of GDP by GTP. Both steps are triggered by the binding of the guanine exchange factor (GEF).(b) Schematic view of the activation of Rab GTPases by detachment of the two geranylgeranyl chains from the membrane and the Rab-GTPase and their transfer to a binding pocket of the guanine dissociation inhibitor (GDI). Image modified after [YuAn 2003]

Membrane anchoring of proteins by specific binding to lipids

Two classes of lipids play a key role for the membrane coupling of proteins through specific forces: the phosphatidylinositols (also called phosphoinositides) exposing two (PIP₂; fivefold maximum charge) and three (PIP₃; sevenfold maximum charge) phosphate groups and the

diacylglycerols generated from PIP2 by phospholipases. The three lipids often serve the transduction of external signals-such as hormones and mechanical forces-into intracellular signals and are thus considered as second messengers. Another lipid involved in the recruitment of proteins to membranes is phosphatidic acid (PA). As shown in Chapter 39 this lipid mediates the electrostatic membrane coupling of the allosteric guanine exchange factor SOS-1 (through the H-domain), together with PIP2 which binds to the PH-domain of the GEF. The generation of the lipids PA and DAG are therefore coupled by the biochemical reaction of the phospholipase PLC- γ and share therefore the same structure of the hydrophobic tails (see Fig. 39.6). There is another pathway of the PA generation which is mediated by the DAG kinase (DAGK).

This subsection deals with the activation of functional proteins by membrane anchoring through lipids acting as second messengers. A major theme is the coupling of different signaling pathways by crosstalk between biochemical reactions of two membrane bound enzymes. One universal mechanism is the generation of a specific lipid anchor by one enzyme which recruits and activates the second enzyme.

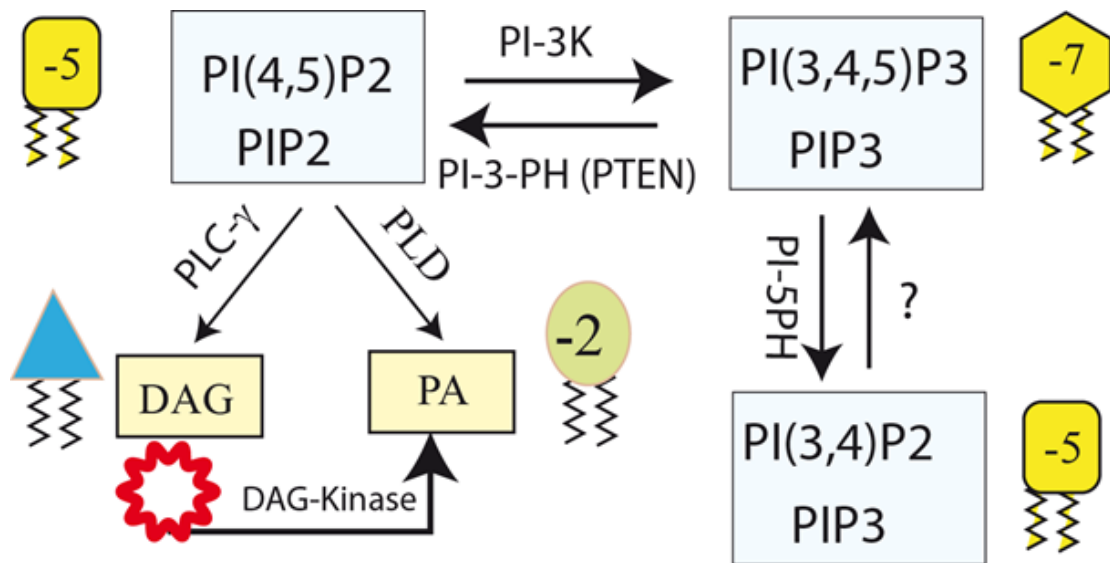


Fig S.9.6: The major functional lipids which act as anchoring sites for functional proteins and simultaneously serve the trans-membrane signal transmission, thus fulfilling the function of second messengers. Please keep in mind that PIPX (X=2 or 3) and DAG are coupled by the phospholipase- γ (PLC- γ and PIPX and PA by the phospholipase D (PLCD))

Phospholipase C- γ (IP3) exhibits the domain structure shown in Fig S.9.7. It plays a central role for the indirect activation of enzymes either by recruitment to membranes through diacylglycerols (DAG) or by rising the intracellular Ca-level. A prominent example is the triggering of the lymphocytes proliferation by encounters with antigen presenting cells which was extensively discussed in the supplemental Chapter 39. PLC- γ activation is mediated by tyrosine phosphorylation in various ways: First, directly by tyrosine kinases (TK) which reside either in the cytoplasm or are coupled to intracellular domains of tyrosin kinase receptors and second, indirectly by coupling to scaffolding proteins and/or membrane bound adaptors. One soluble kinase is Itk (IL2-inducible T-cell kinase) which is activated by SLP-76 after its binding to activated LAT (see Glossar SLP-76). The indirect activation is triggered by coupling of PLC- γ to the activated scaffolding protein LAT which is mediated through SH2 domains.

The lipid mediated membrane anchoring of PLC- γ happens by binding of the PH-domain

(located at the N-terminus) to the phosphoinositides PIP2 and PIP3, but the binding strength to PIP3 is about 50 times stronger than that to PIP2. For that reason the activity of the phospholipase depends on the concentration of PIP3. Therefore the function of the phospholipase is coupled to the activity of the PIP3 generator PI3-kinase as shown in Fig. S. 9 .6.

Very recently it was found that the PLC- γ activating kinase Itk is also bound to PIP3 lipid anchors and that this linkage is enforced by the highly charged inositol tetrakisphosphate (1,3,4,5 IP4) which is generated by phosphorylation of IP3 (see [Huang 2011]). Since this second messenger is generated by PLC- γ the activation of this central enzyme of cell signaling is amplified by the IP4 mediated positive feedback loop.

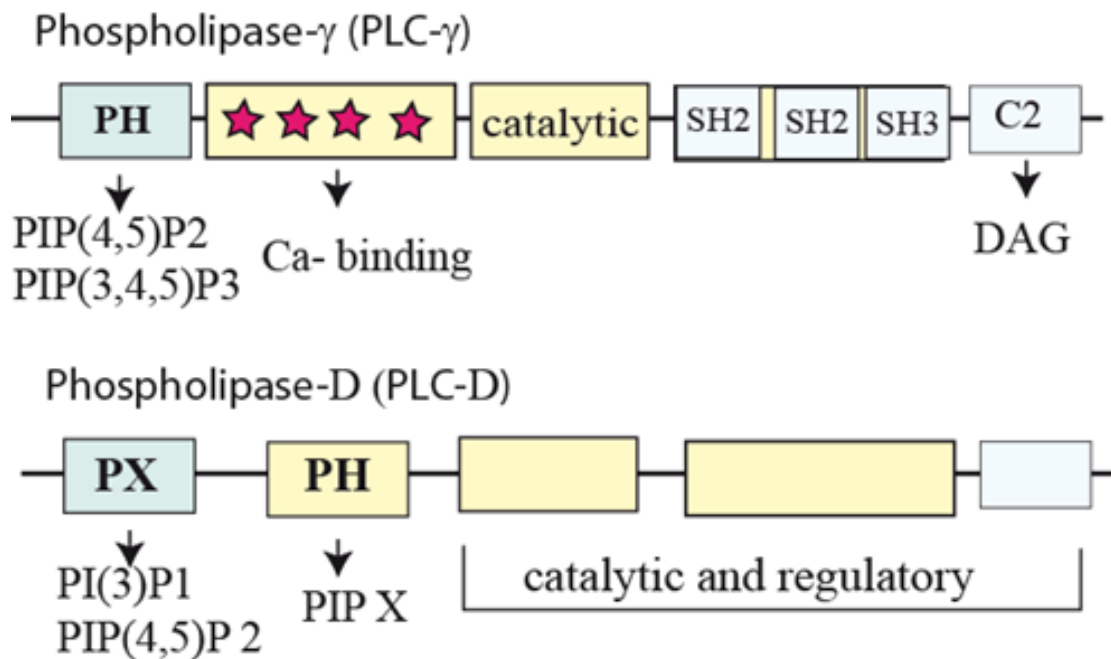


Fig. S.9.7: Top: PLC- γ exhibit PH domains at N-terminus which couple the enzyme to PIP2 and PIP3. PLC- γ binding to PIP3 is at least 50 times larger than to PIP2. Therefore the function of PLC- γ is coupled to the degree of activation of PI-3-Kinase (see below, Fig S.9.9) Bottom: Domain structure of phospholipase D which cleaves the outer phosphate group of phospholipids, thus generating phosphatidic acid (PA) which plays a key role for the membrane recruitment of the guanoside exchange factor SOS (see Chapter 39). Please note that this enzyme exhibits a PHOX (PX) homology domain which binds particularly strongly to the PIP3 (see section on PI-3K below and [Stahelin 2006]))

Phospholipase D (PLD): Catalyses the decomposition of phosphatidylcholines into fatty acid (PA) and choline groups. As shown in Chapter 39, PA can act as lipid anchor for the guanine exchange factor SOS (through the specific histone homology domain). A unique feature of PLD is the PHOX (PX) homology domain at the N-terminus (besides the PH domain) which binds specifically to PIP3, in competition with PH domains [Stahelin 2006]. Moreover, some phospholipase D are also anchored via palmitic acid chains. Remarkable is the relationship between PL-D and the MARCKS protein. MARCKS regulate the activity of PLC-D and of PLC- γ (and

other proteins binding to PIPX) owing to its capacity to sequester the phosphoinositides. The PIPX are liberated by phosphorylation of MARCKS through Protein kinase C resulting in their unbinding from the membrane.

Ca modulated protein binding to diacylglycerol (DAG) anchors

Many proteins involved in the signal transmission across membranes recognize diacylglycerol (DAG) lipids by C1- and C2-homology domains. Please note that the biochemical reactions of enzymes which are recruited to membranes in this way are coupled to the reactions of enzymes generating DAG. According to Fig S.9.6, examples of DAG generators are PLC- γ and DAG-kinases. Most important proteins recruited to membrane by binding to DAG lipids are protein kinase C, PI-3-kinases and its antagonistic PIP3-phosphatase PTEN. The protein binding to membranes enriched in DAG is mediated by C1 and C2 domains. Here we briefly introduce major enzymes bound to DAG by C_i-domains and discuss the modulation of DAG binding by Ca⁺⁺. The readers interested in details on the membrane targeting are referred to reviews by [Cho 2001].

Ras associated proteins. Most members of the small GTPase superfamily Ras bind to membranes by electrohydrophobic forces (see Fig. S.9.1). The same holds for many auxiliary proteins, such as the guanine exchange protein son of sevenless (SOS). Other GEFs bind by coupling to DAGs with the help of C1 domains. An important example is the guanine replacement protein GRP which possesses C1-domains as well as two binding sites for calcium. The binding of the two GEFs (SOS and GRP) by different mechanisms offers several advantages. First the membrane binding of SOS and GRP can be regulated independently. Secondly, the signal transmitted by Ras-GRP can be down regulated by phosphorylation of DAG a process catalyzed by diacylglycerol kinase (DGK).

Phospholipase A (PLA2): Phospholipase A2 (PLA2) plays a key role for the generation of arachidonic acid. It is composed of three domains; a (116 amino acid long) C2-domain at the N-terminus exhibiting two Ca-binding sites, a catalytic domain at the C-terminus and a pleckstrin homology domain at the center which can couple the PLC A to PIP2. The enzyme is activated by translocation from the cytoplasm to the cell envelope in a calcium-dependent manner. Its membrane binding is mediated by two hydrophobic loops which protrude from the C2 homology domain and penetrate into the membrane after Ca-binding (see [Perisic 1999] and [Choh 1999, 2001]).

9.A.3 Activation of and crosstalk between functional proteins by electro-hydrophobic membrane anchoring.

Membrane targeting and activation by C1, C2 homology domains and Ca^{++}

A universal mechanism of membrane targeting of proteins is mediated by C1 and C2 homology domains. They are often present simultaneously (as in PKC) and need in general bivalent ions such as Ca^{++} and Zn^{++} for membrane targeting and activation. A prototype of a protein bound to membranes through C1, C2 and Ca^{++} is the classical protein kinase (cPKC) discussed below. The C1 and C2 domains exhibit similar structures but differ in the following features (see the extensive review by Cho [Cho 1999, 2002]):

- The C1 domain is made up of cysteine rich sequences which are about 50nm long and forming flexible loops (see Fig. S.9.7). The loop tips are sufficiently hydrophobic to induce the penetration into the membranes see Fig S.9.7c). The membrane targeting is accelerated by Ca-ions, but does not depend on it.
- The C2 domain (composed of 130 residues) is more diverse and less selective for lipids. In

general, the Ca^{2+} -dependent C2 domains prefer anionic membranes, in particular PS, but some prefer phosphatidylcholine (such as PLA2-C2).

Calcium plays a twofold role. One is to accelerate the membrane targeting and the other to induce a conformational change that enhances the enzymatic activity. The two steps are kinetically separated. The latter mechanism is similar to the electrostatically induced activation of the guanine exchange factor SOS described in Chapter 39 (see [Cho 1999, 2001]). Binding analyses show that Ca^{++} controls the on-off rate of the C2-domain of PKC. In the presence of $200\mu\text{M}$ Ca^{++} the on-rate is $k_{on} = 1.2 \cdot 10^{10} \frac{1}{\text{Ms}}$ while the off rate is increased by a factor of 100 if calcium is removed. Taken together, these data show that a major role of Ca^{++} is to target the proteins to membranes containing acidic lipids.

Example: Protein kinase C.

Two major classes of membrane associated protein kinase C are known: cPKC (where c stands for classic) nPKC (where n stands for new) and aPKC (where a stands for atypical). cPKC are activated by targeting to DAG and need Ca^{++} , (see Fig S.9. 8) while nPKC require only DAG-lipids. PKCs control the function of many proteins by phosphorylating their serine and threonine residues. It can be activated artificially by phorbolesters which mimic the function of DAG and by increase of the intracellular calcium level (for instance by ionophores). PKC enzymes in turn are activated by all signals inducing an increases in the concentration of diacylglycerol (DAG) or calcium ions (Ca^{++}). Hence PKC enzymes play important roles in several signal transduction cascades. One prominent example is the activation of the transcription of the cytokine interleucine-2 (see Chapter 39 and [Werlem 1998])

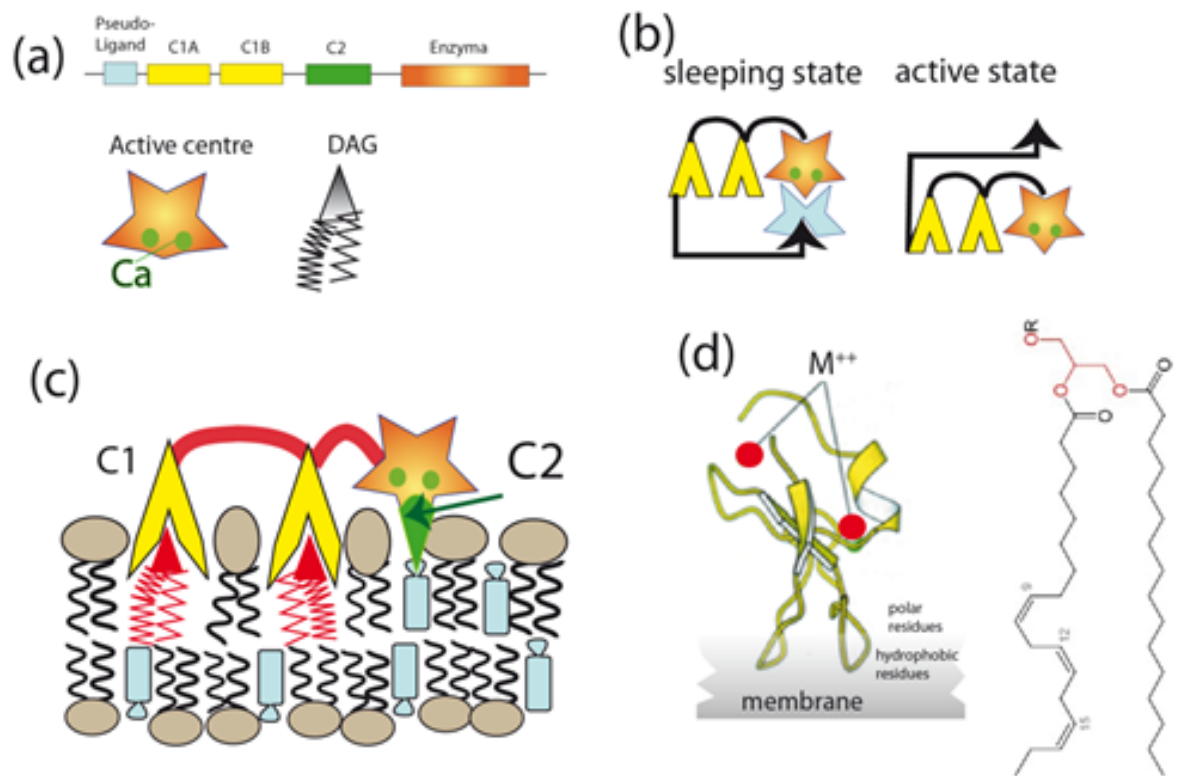


Fig. S. 9.8: (a) Domain structure of protein kinase C (PKC) an example of proteins which bind to charged membranes via C1 and C2 homology domains. (b) PKC is an example of a protein which is kept in a sleeping conformation by binding of a pseudo ligand to the catalytic binding domain and which is activated by membrane binding. (c) Schematic view of membrane binding of PKC by membrane penetration of C1 and C2 domains. Note that C1 binds specifically to DAG lipid. The amino acids sequences just above the membrane surface are polar and those at the tip of the C1 domain are hydrophobic. More detailed structure can be found in [Choh 1999, 2000]. Note that the lipid bilayer is a densely packed liquid crystal and the penetration of C1 domains can be facilitated by the defects of molecular organisation of the lipid bilayer (see [Sackmann 1995]) (d) Molecular structure of the membrane penetrating part of the C1 domain. Please note that the membrane penetrating loop exposes semipolar residues at the region close to the lipid-water interface and hydrophobic at the tip.

Example: Guanine nucleotide releasing protein (GRP): The function of this GTP exchange factor of Ras GTPases has been discussed in Chapter. All Ras-GRP family members contain C1 domains. However, only RasGRP-1 binds to DAG, but not Ras-GRP-2 and Ras-GRP-4. The presence of C1 domains suggests that all RasGRPs could be regulated by membrane translocation driven by C1-DAG interactions. However, all C1 domains of Ras-GRP bind to vesicles containing a high concentration of anionic phospholipids, suggesting that electrostatic forces provide an alternative for recruiting of Ras-GRP to membranes. (see Johnson Biochem. J. (2007) 406, 223-236).

A summary:

Membrane binding via C1 and C2 homology domains play a key role for the activation of many proteins involved in the transmission of external into intracellular signals. Prominent examples are (i) many phospholipases (of the PCLA-, PCLB-, and PCLC-family), (ii) guanine activation factors (GAP) which activate small GTPases by GTP hydrolysis, and (3) phosphoinositol-kinases (PI-3K) and phosphatases (PTEN) discussed below.

Both homology domains bind specifically to diacylglycerols (GAPs), mostly in combination with Ca^{++} . The activation of proteins, binding via C1 and C2, are thus linked to the function of the DAG generator PLC- γ . Many of these proteins are involved in the T-cell activation discussed in Chapter 39. The binding of C1 domains is specifically strengthened by acidic lipid, such as PS, which is possibly caused by Ca^{++} -mediated salt bridges. However, the major binding mechanism of both C1 and C2 rests on the penetration of the two loops into the lipid bilayer. The loop exhibits some amphipathic character, since the amino acids at the roots of the loops are semi-polar while those at the tip are hydrophobic. On the other side, the binding affinity of C1 is rather weak and for that reason proteins expose often two C1-domains and an additional C2-domain, such as PKC [Drieset 2007].

Tandems of antagonistic enzymes: PI-3 kinase and phosphatase

Considering the ubiquitous role of highly phosphorylated phosphoinositols as anchor for functional proteins it is not surprising that many phosphoinositide kinases and phosphatases play pivoting roles for membrane mediated cellular processes such as phagocytosis of pathogens (references see [Sackmann 2010]) locomotion and cell adhesion. We concentrate here mainly on the tandem of enzymes that transforms PIP2 (often abbreviated as PtdIns (4, 5) P2) into PIP3 (PtdIns (3, 4, 5) P3) in a reversible way. The PIP3 generator is phosphoinositide-3-kinase (PI-3K) and the PIP3-annihilator phosphoinositide-3-phosphatase (such as PTEN). The protein binding to PIP2 and PIP3 is mediated predominantly by the two protein homology domains pleckstrin (PH) and PHOX (PX). Since the generators and annihilators of PIPX-lipids play such an important role for the electrostatically mediated membrane recruitment of proteins we describe first some important functions of the PI kinases and PI phosphatases.

The phosphoinositol 3-kinase (PI-3K): membrane binding and activation

The PI-3K, superfamily comprises four classes; IA, IB, II, and III. Each class has unique preferences for phosphoinositide substrates and produces specific lipid second messengers [Vanhaesebroeck 2010]:

1. Class I isoforms are composed of a regulatory and a catalytic section and are activated by $G_{\alpha\beta\gamma}$ coupled receptors and tyrosine kinase receptors. Major functions include cell proliferation, differentiation and locomotion. They are often based on the ability of PI-3K to activate protein kinase B (PKB or Akt) which is due to the activation of these enzymes by binding to PIP2 and PIP3.
2. Class II exhibits only a catalytic section. It catalyses the production of PI (3)P1 and PI(3,4)P2 from PI. Membrane binding is mediated by a C2 domain but most likely without Ca. An isoform

with unique features is PI-3K-alpha. It exposes a PX homology domain with specific membrane binding properties (see below). This enzyme is mainly involved in the clathrin-mediated membrane trafficking and is activated by this coat. It plays also a key role for the exocytosis by neurosecretory granules.

3. Class III is again composed of a catalytic and a regulatory domain and is involved in vesicle trafficking.

The outstanding feature of the class II PI-3K (PI-3K-alpha) is the presence of the PX homology domain which mediates specific and remarkably strong binding to PI (3.4) PIP2 [Stahelin 2006]. The PX domain exhibits a hydrophobic membrane-interaction loop which enforces membrane binding. Similar to the situation for C1, the membrane targeting is mediated by electrostatic attraction while the binding is subsequently enforced by penetration of hydrophobic residues into the hydrophobic region. The PX specificity for PI(4.5)P2 was demonstrated by surface plasmon resonance measurements of binding constants of the PI-3K-II α to neutral membranes (78% PC + 20%PE) containing 2 mole% PIPX. For the full protein $K_d = 20nM$, for the PX-domain alone $K_d = 25nM$ while for the C-domain alone the dissociation constant increased to $K_d \sim 400nM$.

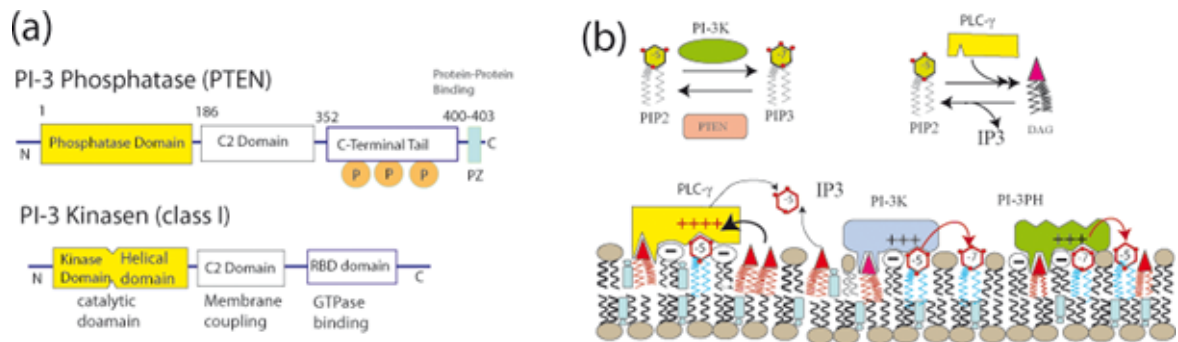


Fig S.9.9: (a) Domain organisation of the two major generators and annihilators phosphatidylinositol 3, 4, 5 phosphate. A common feature is the C2 homology domain while a unique one of C2 is the PDZ domain which mediates the binding to C-terminal domains of other proteins.(b) Schematic view of example of crosstalk of signaling pathways. Shown is the coupling between phospholipase γ , a generator of DAG, and the generators and annihilator of PIP3. The phospholipase generates the lipid anchor DAG which recruits and activates the coupled enzymes.

PTEN membrane binding and activation

Two major phosphatases removing the phosphate 3 are PTEN and SHIP. We concentrate on PTEN which is the most prominent representative and which plays a key role in cancer therapy (see Fig S.9.8)

The PTEN protein consists of an N-terminal phosphatase domain (180 amino acids), a 165 segments lipid binding C2 domain (which is essential for membrane binding), and a 50-amino acid C terminal domain (the 'tail'). PTEN is involved in the regulation of the cell cycle, preventing cells from growing and dividing too rapidly. A unique feature is the high content of phosphorylation sites at the C-end which may play a key role the regulation of its activity and its membrane coupling.

Surface plasmon resonance experiments by Das et al. [Das 2003] show that both the C2 domain

Lipid mixture	Protein	$K_d[M]$	$k_{off}[s^{-1}]$
CLPM: PC/PE/PS/PI/Ch.(12:35:22:9:22)	Wild type	$1 \cdot 10^{-9}$	$1.5 \cdot 10^{-3}$
CLNM: PC/PE/PS/PI/Ch. (61:21:4:7:7)]	Wild type	$> 10\mu M$	Not measurable
Model composition PC/PS 80:20	Wild type	$3 \cdot 10^{-9}$	$1.5 \cdot 10^{-3}$
	C2 domain	$9 \cdot 10^{-8}$	$2 \cdot 10^{-1}$

Table I: On the electrostatic-hydrophobic PTEN binding to natural lipid compositions of cytoplasmic leaflet (CLPM) of plasma membrane and nuclear membrane (CLNM), respectively [Das 2003]. All hydrophobic tails were oleyl chains. Note first, that effect of cholesterol (Ch) is negligibly small and second that binding strength reduced 80 fold at 400mM KCl. Note that the binding constant of Ca^{++} is $K_d = 2\mu M$.

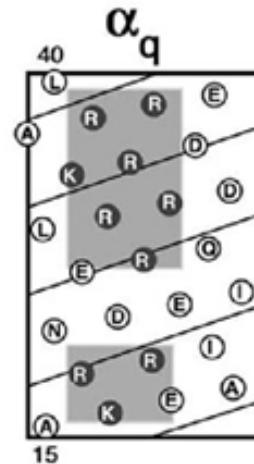
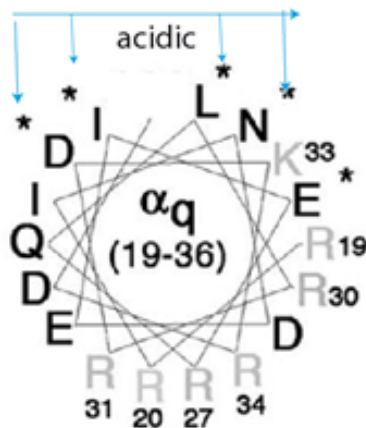
and the phosphatase domain contributes to the electrostatic membrane binding of PTEN since both domains exhibit clustered cationic residues, although no fatty acid chain. The C2 domain has only few binding sites for Ca^{++} and therefore C2-mediated binding may be Ca-independent. Most importantly, the affinity of the C2 domain for POPC/POPS (8:2) vesicles was ≈ 30 times lower than that of the full-length PTEN, suggesting that the C2 domain itself is not critically involved in membrane binding of PTEN. Another interesting finding is that binding of PTEN to the nuclear membrane containing only 15% charged lipids is extremely weak (K_d is of the order of μM) Finally, it is essential to note the electrostatic binding is non-specific since it does not depend appreciably on the type of the charged lipid.

Heterogeneous $G_{\alpha\beta\gamma}$ mediated membrane processes. In Kapitel 9 we introduced the function of these heterogeneous GTPases as hormone or photon amplifier. In Kapitel 28 we discussed the

self-assembly and activation of intracellular micromuscles by hormone-mediated activation of $G_{\alpha\beta\gamma}$ (see Fig 28.4). Finally these molecular switches play also a key role for the regulation of the locomotion of cells (such as Dictyostelia) by gradients of the chemoattractant c-AMP. In all cases the activation is triggered by replacement of GDP by GTP which is initiated by coupling of the intracellular domain of the hormones to the GTPases resulting in the detachment of the G_α domain. Both fragments: G_α and $G_{\beta\gamma}$, are functional. The major function of G_α is the activation of adenylate cyclases (the generator of c-AMP from ATP in the case of Dictyostelia) and the decomposition of phosphor diesterases (in the case of vision, see Kapitel 9). The activation of the adenylate cyclase occurs in combination with CRAC, a cytosol residing protein exhibiting a pleckstrin domain coupling the enzyme to PIP2 or PIP3. While G_α activates adenylate cyclase and phosphor diesterases the unit $G_{\beta\gamma}$ is involved in the activation of ion channels and phospholipases.

The G_α activation is another example of the electro-hydrophobic protein recruitment to membranes also coupled to acidic membrane via polybasic sequences. Membrane targeting is mediated by myristoylation or palmitoylation together with electrostatic forces. The helix of the G_q unit exposes two charged surfaces. One exhibits clusters of negatively charged amino acids (shown in the wheel model of Fig S.9.10) which mediate the binding to the $G_{\beta\gamma}$ unit. The other surface exposes a large positively charged patch comprising altogether 10 basic amino acids. Experiments by Crouthamel et al [Crouthamel 2008] showed that replacement of the basic units by acidic ones abolishes membrane targeting.

α_s MGCLGNSKTEDQRNEEKAQREANKKIEKQLQKDKQVYRATH



It is important to add a note of caution. Removal of the basic units can be overcompensated by myristoyl groups. In fact, to abolish the membrane binding of the G_q unit nine basic residues had to be replaced. It could be recovered if a myristoyl chain was introduced by mutations.

On the nucleation growth and stability of membrane domains-Two routes to domain formation

Motivation of this section: Microdomains are often called rafts. This name does not do justice

to their function as nano-scale reaction platforms assembling distinct enzymes, regulatory proteins (inhibitors or activators) and lipids within fluid multi-component mixtures. Paradigms of such localized reaction platforms are immunological synapses (see [Dustin 2005] and [Sackmann 2011]) and the adhesion domains acting as nuclei of actin growth and clutches mediating the momentum transmission to substrates during cell locomotion [Sackmann 2010]. We saw that the microdomains are highly dynamic and transient entities which are initiated by enzymes (such as phospholipase- γ) generating lipid anchors such as diacylglycerol, phosphatidic acids or phosphoinositides which serve as nucleation sites for the recruitment of other enzymes. In this way two or several enzyme reaction could be coupled by positive or negative feedback loops. Thus, different signaling pathways that are triggered by such coupled enzymes would be temporally synchronized. An example is the activation of the MAPK and NFAT mediated pathway of genetic expression discussed in Chapter 39.

Most remarkable is the large number of different enzymes which are recruited to membranes and activated by binding to diacylglycerols, such as phospholipases. After fulfilling their function the microdomains are internalized and dismantled, such as the immunological synapses. This could serve the down-regulation of the signaling processes or the removal of the highly insoluble DAG lipids, but also the homeostatic control of the membrane composition and structure as well, an aspect considered more closely below.

The experiments summarized in this Chapter and Chapter 39 showed that the lipid/protein clusters nucleate within seconds at random sites and grow only to a size of $\sim 1\mu m$. As we saw in Chapter 39 a likely reason is the small number of proteins involved (typically 10^4 per cell) and the simultaneous formation of many domains. There are two routes to domain formation in membranes. One is the classical nucleation and growth process which could be triggered by switching the membrane into a state of phase coexistence, which could be achieved by changing the temperature, the osmotic pressure or the lateral membrane tension (see Kapitel 12). The second route is mediated by adsorption of proteins via electro-hydrophobic forces.

The domain formation through the first route could be described in terms of a modified nucleation and growth theory developed by I. Lifshitz and C. Wagner for droplet formation in supersaturated vapours. The theory was modified for fluid-solid mixtures in numerous papers (see [Wu1998] and [Madras 2001]). A theory for two dimensional mixtures is still missing due to the difficulties to solve the diffusion equation in 2D (see Appendix A of chapter 39). We therefore consider here the thermodynamic model of the rate of nucleation to gain insight into the parameters controlling this process.

Consider a circular microdomain of radius R enriched in the lipid component A (which could be DAG) embedded in a reservoir of fluid lipid B. The energy cost to generate a lipid domain of radius R can be expressed as:

$$\Delta G = -\pi \left(\frac{R}{a} \right)^2 \Delta \mu_A + 2\pi R \Gamma$$

(S.9.7)

Where $\Delta \mu_A$ is a measure for the energy per molecule, gained by the transition of the system into the state of phase coexistence. Γ is the line tension which is a measure for the work required to remove a lipid A from the rim of the domain to the bulk phase (with the dimension of force or of energy per unit length). It is in general not known. Eq. (S.9.7) predicts that for small radii ΔG is positive since the gain in binding energy per molecule (determined by the first term) is smaller than the interfacial energy cost per molecule. Clearly the domain will grow above a critical radius R^* .

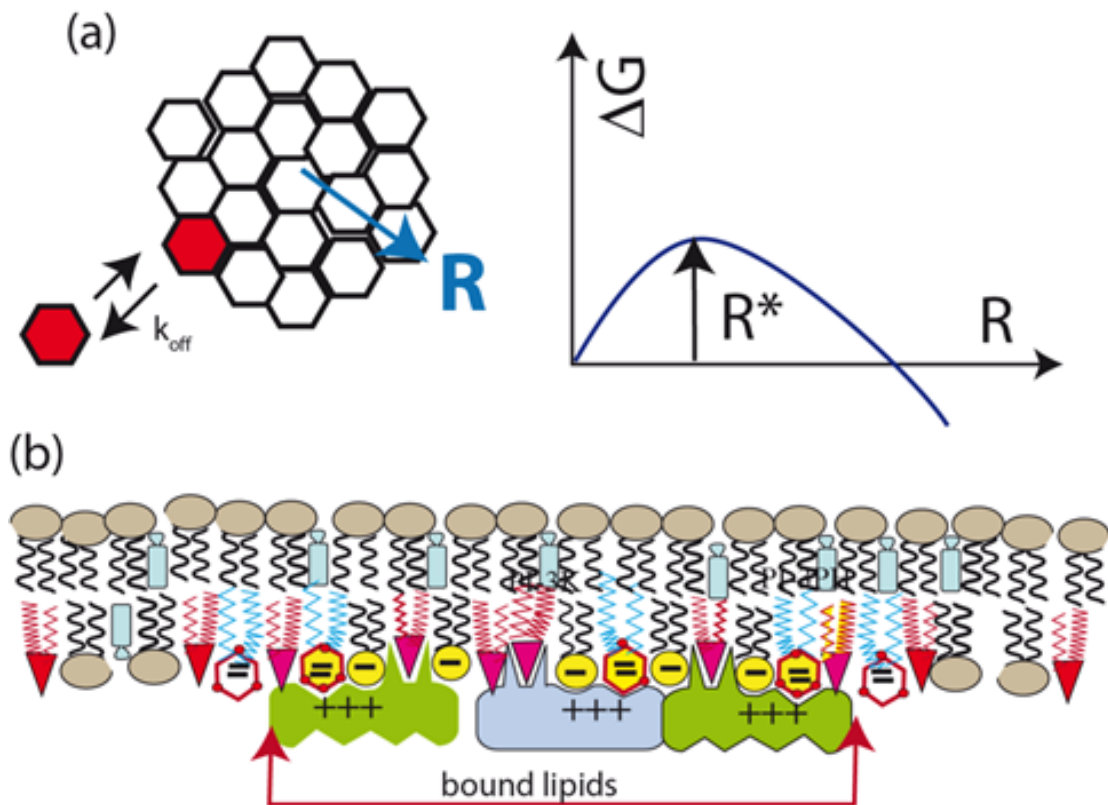


Fig S.9.11: (a) Left: lateral distribution of lipids within C2 domains. Right: Change of free energy of lipid cluster with the size of the domain radius R and definition of critical radius R^* . (b) Cartoon of microdomain enriched by charged lipids and diacylglycerol which is stabilized by protein binding. Note that the domain is thermodynamically metastable as long as the proteins remain bound.

The critical radius is determined by the maximum of the free energy. A simple calculation yields for the critical radius:

$$R^* = \frac{a^2 \Gamma}{\Delta\mu} \quad (\text{S.9.8})$$

Now we address the question which factors influence the nucleation rate of clusters of the critical radius R^* . If domains are formed by a sudden change in temperature (or pH) until phase separation in two phases α and β sets in, the classical theory of homogeneous nucleation holds (see [Cahn-Haasen 1983] Chapter 9). The number of nuclei of the high melting phase α of radius R (enriched in the high melting component A) is determined by the Boltzmann law: $n_i = n \exp \left\{ \frac{-\Delta G}{k_B T} \right\}$, where n is the number of molecules per unit area of the phase α and ΔG is the energy given by (S.9.7). The number of nuclei of the critical size is obtained by replacing ΔG by ΔG^* which is obtained by inserting R^* into equation (S.9.7) yielding:

$$\Delta G^* = \pi \frac{\Gamma^2 a^2}{\Delta \mu}$$

(S.9.9)

Note, that $\frac{\Delta \mu}{a}$ is the melting energy per area occupied by one lipid molecule. In addition, the growth rate is determined by the diffusional jumps of the molecules A at the rim of the disc which can be expressed by the Einstein relation: $\nu_j = 4D a^2$. According to the free area model of diffusion presented in Kapitel 10, the lipid diffusion in fluid membranes can be expressed in terms of an Arrhenius law with an effective activation energy: ΔG_L^* ; $\nu_j = \nu_0 \exp \frac{-\Delta G_L^*}{k_B T}$. Here ν_0 is the jump frequency of the lipid molecules within their solvent cage as defined in the free volume model (references see [Sackmann 1995]). The rate of nucleation can now be expressed as:

$$I = \frac{1}{4} n_L^* \nu_0 n_A \exp \left\{ - \frac{\Delta G_L^* + \Delta G^*}{k_B T} \right\}$$

(S.9. 10)

In the case of homogeneous nucleation induced by changing the temperature (or the pH and

ionic strength in the case mixtures containing charged lipids), the chemical potential $\Delta\mu$ can be replaced by $\frac{L\Delta T}{T_0}$ where L is the heat of melting per area a^2 (see Eq. S.9.7) and ΔT is the supercooling which is determined by the distance between the liquidus line of the fluid-solid phase boundary and the observation temperature T_o (see [Cahn-Haase 1983]).

To get an impression of the exponential factor let us consider now a few numbers. At present there is no way to obtain a good estimate of the prefactor and we consider only the activation factor by considering few numbers.

The heat of melting of lipids is $L \sim 40 \frac{\text{kJ}}{\text{mole}}$ ($\sim 15k_B T$ per molecule or nm^2), the apparent activation energy of the lipid diffusion ($\sim 5k_B T$) resulting in an Arrhenius factor of $e^{-20} \sim 10^{-9}$. This factor is essentially compensated by the local jump frequency of the lipids which is of the order of 10^8 Hz and the nuclei are thus expected to form in the time scale of seconds. The supercooling ΔT is of the order of 10°C and $\Delta T/T \sim 0.1$. The line tension is also of the order of ΔL (but smaller since the lipids at the rim of the domain are more weakly bound than those in the center) and our estimation yields $R^* \leq 100a = 100\text{nm}$ which is not far from observed domain sizes in the μm regime.

In the following we address two unsolved questions. A long standing unsolved question of membrane physics is whether the thermodynamically driven nucleation and growth is biologically relevant and why the domains formed in mixed lipid membranes and monolayers are stable over long times. In fact, the same question bothers Chemical Physicists since the introduction of the concept of nucleation and growth (Oswald ripening) by Oswald and the Kelvin-Gibbs-model of vapor droplet formation [Wu 1998]. The time evolution of nucleation and growth can be successfully described by the Lifshitz-Slyozov-Wagner (LSW) theory for three dimensions, which predicts that the radius of the precipitations, R , growth very slowly as $R(t) \propto t^{1/3}$. The model can also explain the formation of stationary states with rather small size distributions. More recently, the nucleation and growth problem has also been solved for two dimensional systems [Zeng 1989] and it was shown that the same power law $R(t) \propto t^{1/3}$ holds also in 2D. While there

are numerous theoretical studies experimental verifications of the theory are still missing. Model membrane studies could be helpful to test the models.

On the biological relevance

A controversially discussed question is whether the nucleation and growth of microdomains by thermodynamically driven lateral phase separation is biologically relevant. The answer is most likely no. In the resting state of cells swimming in the body fluid without being subjected to external cues, the average composition of the multicomponent lipid-protein-mixture of the plasma membrane is well controlled. The equilibrium composition is controlled both during the membrane biosynthesis in the ER and by posttranslational modifications in the intracellular compartments together with lipid exchange proteins (see Chapter 9 and Kapitel 12, Figure 12.7). The lipid composition is generally adjusted to the local environmental temperature. The fraction of unsaturated lipids is increased in body regions constantly exposed to low temperatures, such as in the lower parts of reindeer legs. The lipid composition can also be adjusted to temporal temperature changes, a capacity playing a key role for the cold resistance of plants [Welti 2002].

The homeostatic control of the membrane composition after changes induced during the activation of cells, such as locomotion, growth processes or lymphocyte activations, is maintained by constant recycling of the lipids and proteins through exocytosis and endocytosis, which has to be accompanied by lipid and protein sorting. The main purpose of the present Supplementary Chapter S.9 and Chapter 39 is to show that the formation of functional microdomains is predominantly mediated by adsorption of functional proteins driven by electrostatic forces and the hydrophobic effect. The generation of immunological synapses by cell-cell adhesion is triggered by the membrane adsorption and activation of the phospholipase- γ is a paradigm of microdomain formation. The pace maker enzyme PLC- γ generates the DAG lipids and Ca^{++} bursts which mediated subsequently the adsorption of auxiliary proteins such as protein kinase C, phospholipase D and the guanine exchange factors. (see Fig 39.10 and 39.11). A challenging question is whether the nucleation rate is delayed by the sequestering of the negatively charged

lipids by the MARCKS protein [McLaughlin 2000].

The growth kinetics of the microdomains is determined by the rate of DAG generation, and the rate of adsorption of the proteins binding to this lipid anchor (such as protein kinase C, PI-3K and PI-3PH or phospholipases exposing C1 and C2 domains). As shown in the discussion of the Smolukowsky equation (see Chapter 39. Appendix A) the growth rate of the domains determined by the lipid diffusion is very fast and is most likely not rate limiting.

There is another specific feature of micro domain formation in cell membranes. The solubility of the DAG lipids in fluid bilayers is low (of the order of 10%). Since there is no thermodynamic restoring force, the lifetime of the microdomains could be very long. In order restore the optimum composition of the plasma membrane and to down-regulate the activity of the reaction centers, the microdomains must be continuously internalized by endocytosis, through coated pits and caveoli. This occurs in the SMACs which coexist with the immunological synapses. Due to the separation of the global reaction platform (SMAC) and IS the process of T-cell activation can go for many hours.

9.A.4 S.9.Appendix A

Appendix A: On the fast dynamics of lipid reorganization of membranes by electrostatic lipid-protein interaction.

A.1: Reminder of the electrostatics of membranes

In Kapitel 11 we dealt with the effect of charged lipids on the lateral surface pressure and phase transitions of membranes based on the linearized Poisson Boltzmann (PB) equation. This simple

model provides useful information on the modification of lipid phase transition by pH changes and ionic strengths of the aqueous phase [Jähnig 1990], [Sackmann 1995]. For the theoretical treatment of the localized electrostatic interaction of proteins with membranes containing highly charged lipids such as PIP2 and PIP2 more sophisticated theoretical models based on the solution of the non-linear PB-equation are required [Andleman 1997] [Harries 1998]. The total free interaction energy of a charged polymer with the membrane is determined by three contributions:

$$G = G_{el} + G_E + G_P$$

(A.1a)

The first term stands for the electrostatic interaction, while the second and third account for the translational entropy of the salt and lipid, respectively. The electrostatic energy is given by the equation:

$$G_{el} = \frac{1}{2} \epsilon_0 \epsilon_w \left(\frac{k_B T}{e} \right)^2 \int \int (\nabla \Psi)^2 dV$$

(A.2a)

Where Ψ is the reduced electrostatic potential: $\Psi = \frac{e\Phi}{k_B T}$. Please note that this equation follows from the classical equation for the potential energy $U(E)$ of the electric field:

$$U(E) = \frac{1}{2} \epsilon_0 \int_V \vec{E} \cdot \vec{D} dV$$

The Euler Lagrange equation of the energy functional yields the nonlinear Poisson Boltzmann equation of the electrified surfaces:

$$\Delta\Psi = \lambda_D^2 \sin^2\Psi \text{ with } \lambda_D = \sqrt{\frac{\epsilon_0 \epsilon_w k_B T}{2e^2 c_0}} \quad (\text{A.2b})$$

where $\lambda_D = \kappa^{-1}$ is the Debye length.

By considering that the aqueous phase contains only monovalent salt we can express the translational entropic free energy of the electrolyte by:

$$G_E = k_B T \int_V dV \left\{ n_+ \ln \frac{n_+}{n_0} + n_- \ln \frac{n_-}{n_0} - (n_+ + n_- - 2n_0) \right\} \quad (\text{A.2c})$$

n_+ and n_- are the numbers of anions and cations, fulfilling the condition $n_+ + n_- = n_0$. Finally, the two dimensional mixing entropy of the mobile lipids is given by:

$$G_L = \frac{k_B T}{a} \oint_V dV \sum_i^m x_i \ln x_i \quad (\text{A.2d})$$

These equations have to be solved by considering the boundary conditions of material conservation for the lipids: $\sum_1^m x_i = 1$. The charge density of the membrane can be expressed as :

$$\sigma = \frac{e}{a} \sum_1^m z_i x_i \quad (\text{A.3})$$

Here it is assumed that the pH and the ionic strength are constant. If structural changes of the membrane are mediated by changes of the pH or the ionic strength, the charge e has to be replaced by $q = \alpha e$, where α is the degree of dissociation (see Kapitel 10.2.3)

Based on these energy functions, Daniel Harries and coworkers have numerically calculated the kinetics of the reorganization of the distribution of charged lipids induced by the adsorption of globular proteins (macroion) and flexible polybasic polypeptides [Khelashvili 2008].

The basic equation accounting for the in-plane flux $j_i(\vec{r}, t)$ of a lipid species i can be expressed as:

$$\frac{\partial x_i(\vec{r}, t)}{\partial t} = -\nabla \cdot j_i(r, t)$$

(A.4)

The lipid motion is similar to the trans-membrane flux j_i of ions through membranes which has been treated in Kapitel 14 for the calculation of the stationary potential of nerve cell membranes.

$$j_j = -\frac{1}{N_L} \cdot u_j c_j \cdot \left(RT \frac{\partial \ln c_j}{\partial x} + z_j F \frac{\partial \Phi}{\partial x} \right) \text{ and } u_i = \frac{D}{k_B T}$$

(A.5)

D is the diffusivity of the lipids. Since we use molar fractions instead of concentrations we obtain for the tangential flux of lipids:

$$\frac{\partial x_i(\vec{r}, t)}{\partial t} = \frac{D_i}{k_B T} \text{grad} [x_i(r, t) \text{grad} \mu_i(r, t)]$$

(A.6)

where μ_i is the chemical potential of the lipid and x_i can depend on time and space. The reader familiar with the dynamics of phase separation in synthetic materials (such as metal alloys) will recognize the similarity of equation (A.6) with the Cahn Hilliard theory of spinodal demixing (see Kapitel 12 and [Sackmann 1995]). As discussed in Chapter 39 the above model has been applied to evaluate the energetics of the electro-hydrophobic coupling of polybasic proteins to acidic membranes. Below we discuss the application of the equations (A3) to (A.6) to study the kinetics of macromolecular adsorption to membranes. The basic method was developed in pioneering work by the Andelman group [Andelman 1997] to study the kinetics of the surfactant self organisation at the fluid-fluid interfaces.

On the kinetics of lipid accumulation below polybasic proteins

The above set of equations was applied by the Harries group to evaluate the time evolution of the lipid reorganization induced by the sudden adsorption of basic proteins at the membrane surface [Khelashvili 2008]. The technique enables valuable insights into the kinetics of charged lipid accumulation beneath the polybasic macromolecules. It has also been applied to evaluate power laws of the non-Brownian diffusion of lipids which are electrostatically coupled to the proteins. As an example we discuss the control of the lipid distribution by the balance of electrostatic and entropic forces in a biological relevant mixture containing 10mole % PS and 1mol% PIP2. Insight in this balance can be gained without detailed calculations by comparing the chemical potentials of the lipid molecules in the bare membrane region μ_i^α and a protein covered domain μ_i^β .

$$\mu_i^\alpha = k_B T \ln x_i^\alpha + z_i e \Phi_i^\alpha \text{ and } \mu_i^\beta = k_B T \ln x_i^\beta + z_i e \Phi_i^\beta$$

(A.7)

These equations are obtained by calculating the chemical potential from Eq. (A.3) according to $\mu_L^\xi = \mu_i^\xi + \frac{\partial G_L}{\partial N_i}$ and by making three assumptions: first, that the standard chemical potentials are the same in the two phases; second, that the molar fraction of the charged lipids are small ($x_i \ll 1$) while that of the non-charged is close to one, third, that the lipid distributions in the two phases α and β is homogeneous [Khelashvili 2008]. The second term of each equation accounts for the electrical energy of the lipids in the Gouy Chapman potential of the membranes. Below we consider two enlightening result of the Monte Carlo experiments.

Fig S.9.A.1a compares the excess distribution of the PS and PIP2 lipids (normalized by the average distribution) beneath an ion deposited on the membrane surface after 400 nsec. Both lipids accumulate beneath the ion, but the excess concentration of the highly charged PIP2 lipid is by

a factor of 5.5 higher than that of the monovalent lipid. Fig S.9.A.1b shows that the accumulation is realized within 50 nsec. This is considerably faster than expected for a purely diffusive process. The average distance of the PIP2 from the macro-ion is $\delta \approx 10\text{nm}$ and the time for the nearest PIP2 molecules reaching the ion by random walk would be $t \sim \delta^2/2D \approx 5 \times 10^{-7}\text{ sec}$, which is about an order of magnitude slower than the time ($4 \times 10^{-8}\text{ sec}$) observed in Fig. S.9.A.12. This discrepancy suggests that the reaction is accelerated by tangential electric force exerted by the ion.

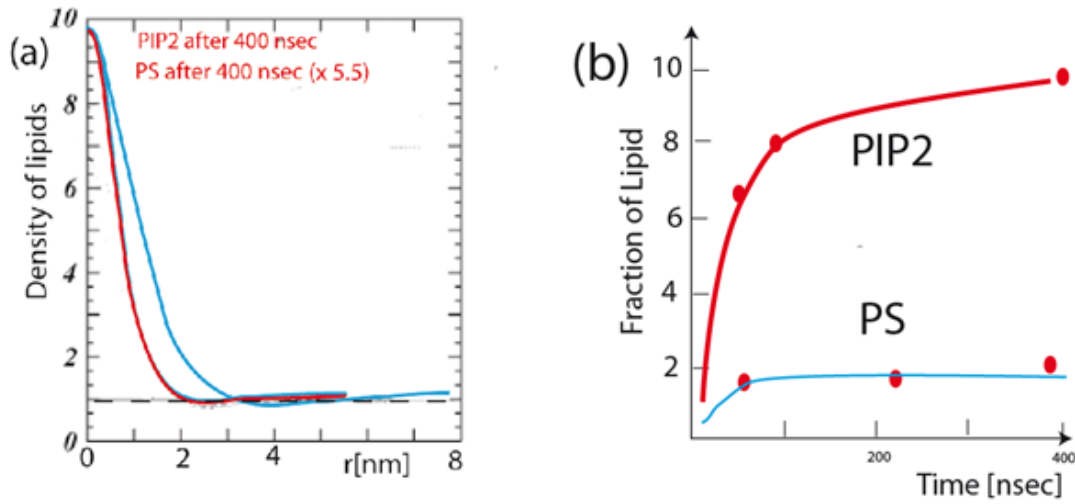


Fig. S.9.A.1 (a) Excess lateral density distribution of PS and PIP2 beneath a positively charged spherical macro-ion of 2nm diameter, 400 nsec after placing the ion on the surface. Note that the amplitude of the PS distribution is increased by a factor of 5.5. (b) Monte-Carlo simulation of time evolution of PIP2 and PS accumulation beneath macro-ion. The data points were obtained from the amplitudes of the excess lipid distributions calculated for different times after ion deposition (see Fig 3 in [Harries 2008]).

Fig S.9.A.2c shows another intriguing computer experiment which sheds new light on the modulation of molecular motions in charged lipid membranes by medium range electrostatic interactions. Since adsorbed ions can move faster than lipids, the lateral diffusion of charged lipids is modulated by the ion diffusion and vice versa. Each diffusional jump of the ion induces the reorganization of the cloud of the surrounding charged lipids. In Fig.S.9.A.2c the mean square

displacement of an ion adsorbed to a ternary mixed membrane containing 20% PS and 1% PIP2 is plotted as a function of time by assuming that the diffusivity of the ion is 10 times larger than that of the lipids. The coupling of the diffusion of the ion and the lipids leads to characteristic deviations from the classical Einstein law $\langle x^2 \rangle \approx t$. The effect of the highly charged PIP2 is particularly large. The ion motion is slowed down considerably since any motional jump is impeded by the electrostatic trap created by the sequestered PIP2. The effect is similar to the slowing down of the ion motion in electrolytes by the Onsager Retardation field.

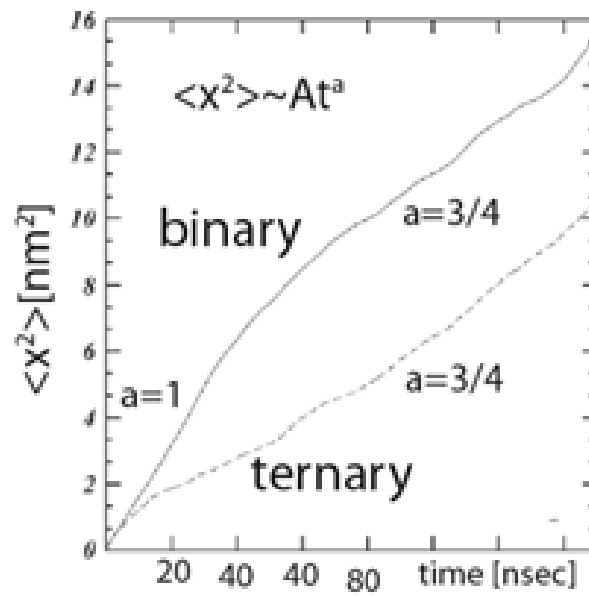


Fig. S.9.A.2c: Monte Carlo simulation of time dependence of the mean square displacement $\langle x^2 \rangle$ of the macro-ion adsorbed on membranes containing 20% PS and 1% PIP2. The diffusion coefficient of the ion is assumed to be 10 times larger than that of the lipids. The exponents a of the power law $\langle x^2 \rangle \propto t^a$ are obtained from double logarithmic mean square displacement-vs-time plots.

Concluding Remarks:

An important prediction of the Monte Carlo experiments is that a low concentration of the PIP2, compared to the monovalent PS, is compensated by the higher charge. Typically the inner leaflets

of plasma membranes and the outer monolayer of cytoplasmic organelles contain 10% of PS (with $z_{PS} = -1$) and only 1% of PIP2 (with $z_{PIP2} \sim 3 - 4$ at pH 7). According to Eq. (A7) the entropic contributions are $-2.3k_B T$ and $-4.6k_B T$, respectively. The surface potential can be estimated according to:

$$\Psi_0 = \frac{2 k_B T}{e} \arcsin h \left(\frac{1,34 \alpha}{A \sqrt{c}} \right)$$

, where α is the degree of dissociation, A is the area per lipid in nm^2 and c is the ionic strength in $\frac{M}{l}$. For the free monolayer containing 10 % PS- and $c \approx 200mM$ we obtain $\Psi_0 \approx 150 mV$. Thus the gain in electrostatic energy by transfer of a molecule from the free membrane to the protein covered domain is of the order of $e\Psi_0 \approx 100 meV$ for a PS molecule and 300 -500 meV for PIP2 (corresponding to $2.5k_B T$ and $7.5 - 12k_B T$, respectively). The major message of this rough estimation is that the decrease in concentration of the charge component can be easily compensated by the gain in electric energy if the charge is increased. The reason for the dominance of the electrostatic energy over the entropic is the logarithmic dependence of the entropy on concentration. For PIP3 the surface charge is increase to about $z = -5$. The average concentration is 0.1%. Compared to PIP2, the entropic energy costs increase by a factor of 1.5 while the electrostatic energy gain in increases by a factor of 1.5. This estimation shows that the electrostatic interaction energies between lipids and proteins can be finely balanced by cells through the control of charge and concentration. The interaction of PIP2 and PIP3 with membranes may be further enforced by the formation of several hydrogen bonds between their phosphates and lysine groups of the protein (see Figure S.9.3).

9.A.5 Supplementary Information

Appendix A

Abbreviations:

PKC: protein kinase C

PLA2: phospholipase A2

cPLA2 cytosolic phospholipase A2

DAG diacylglycerol

PI3K phosphatidylinositol -3-kinase

PI3P phosphatidylinositol -3-phosphatase

PLC- γ : phospholipase-gamma

Appendix B

PHOX (PX)-homology domains. Several important enzymes involved in signal transmissions at membranes carry PX-domains which bind to phosphoinositides PIP2 and PIP3. Two prominent examples are the phospholipase D (PLD) and some phosphoinositide 3-kinase, such as PI3K-C2a.

The PX mediated protein binding is much stronger to PIP2 than to PIP3, in contrast to the PH-domain. Structural and membrane binding analyses show that the membrane binding of the PX domain is initiated by nonspecific electrostatic interactions followed by the membrane penetration of hydrophobic residues. PX domain displayed higher PIP2 mediated binding affinity than C2 domain. Dissociation constants: PI3K-C2a-PX: $K_d = 20nM$. PI3K-C2a-C2: $K_d = 0.5\mu M$. Reference: Stahelin, RV. et al. (2006) Structural and membrane binding analysis of the Phox homology domain of phosphoinositide 3-kinase-C2alpha. J Biol Chem. 281: 39396-39406.

Appendix C

Small GTPases and functions

Name	Function	Functions described
Ras	Cell proliferation	T-cell activation ; Ch 39
Rho, Rac,Cdc 42	Cytoskeleton reorganisation	Formation intracellular muscles, Filipodia formation
Rab	Membrane trafficking	Fig S.9.6
Rap	Cell adhesion	
Arf	Vesicle transport	
Ran	Nuclear transport	

9.A.6 References

[Ben Shaul 2008] Tzlil S. Murray, D., Ben Shaul, A. (2008) The electrostatic switch mechanism: Monte Carlo Study of MARCKs-Membrane interaction. Biophys. J. 95:1745-1757

[Cahn-Haasen 1983] R.W. Cahn and P. Haasen. Physical Metallurgy. North Holland, Amsterdam 1983.

[Cho 1999, 2001] (a) Cho, W. (2001) Membrane Targeting by C1 and C2 Domains J. Biol. Chem. 276:32407-32410. (b) Medkova, M., Cho, W. (1999) Interplay of C1 and C2 Domains of Protein Kinase C: Membrane Binding and Activation. J. Biol. Chem. 274: 19852-19861

[Conibear 2010] Conibear, E., Davis, N. 2 (2010) Palmitoylation and depalmitoylation dynamics at a glance J. Cell Sci. 123, 4007-4010.

[Crouthamel 2008] Crouthamel, M. et al. (2008) N-terminal polybasic motifs are required for plasma membrane localization of Galpha(s) and Galpha(q). Cell Signal 20:1900-10.

[Das et al 2003] Das, S. (2003) Membrane-binding and activation mechanism of PTEN. PNAS 100, 7491-7496

[de Gennes 1997] De Gennes, PG. Scaling Concepts of Polymer Physics, Cornell Univ. Press 1979

[Dibbie 1996] Dibbie, A., et al. (1996) Lipid lateral heterogeneity in PC/PS/DAG vesicles and its influence on protein kinase C. Biophys. J 71: 1877-1890.

[Dries 2007] Dries, DR., et al. (2007). A single residue in the C1 domain sensitizes novel protein kinase C isoforms to cellular diacylglycerol production. J. Biol Chem. 282:826-830

[Dustin 2004, 2005] (a) Yokosuka T et al. 2005 Newly generated T-cell receptor microclusters initiate and sustain T-cell activation by recruitment of ZAP-70 and SLP-76 Nat. Immunol. 6: 1253-62. (b) Varma, R. et al. (2006) T-cell receptor proximal signals are sustained in peripheral microclusters and terminated in the central supramolecular activation cluster Immunity 25: 117-27.

[Evans 1999] Evans E. and Ludwig F., (1999) Dynamic strength of molecular anchoring and material adhesion in cohesion in fluid biomembranes. J. Condensed Matter 11: 1-6

[Gerke 2002] Gerke, V., and Moss, S. E. (2002) Physiol. Rev. 82, 331-71

[Hancock 1990] Hancock, JP. (1990) A polybasic domain or palmitoylation is required. Cell. 63: 133-139.

[Hancock2003] Hancock, JP. (2003) Nature Reviews Molecular Cell Biology 4, 373-385 (May 2003)

[Hiemenz P.] Principle of Colloid and Surface Chemistry M Dekker New York Basel 1986

[Houtman 2005] Houtman, JR. et al (2005) Early Phosphorylation Kinetics of Proteins Involved in Proximal TCR-Mediated Signaling Pathways. J. of Immunology. 175: 2449-2458

[Huang 2011] Huang YH. Sauer K. (2011) Lipid signaling in T-cell development and function. Cold Spring Harb. Perspect. Biol. 2010; 2:a002428

[Komura Andleman 2004] Komura, S., et al. (2004) Lateral phase separation in mixtures of lipids and cholesterol. Europhys. Letters 67: 321-327.

[McLaughlin 2002] McLaughlin, S., [2002] PIP2 and proteins: Interactions, organization and information flow. Annu. Rev. Biophys. Biomol. Struct. 31:151-75

[Mouritsen] M. Jensen and Ol. G. Mouritsen (2004) Lipids do influence protein function-the hydrophobic matching hypothesis revisited. Biochim. Biophys. Acta 1666: 205-226

[Moy 2003] Wojcikiewicz, E., et al (2003) J. Cell Sci. 116: 2531-2539

[Netz 1999] Netz, RR. (1999) Debye-Huckel theory for interfacial geometries. Phys. Rev. E 60:3174-3182.

[Nielssen 1999] Nielsen, E., (1999) Rab5 regulates motility of early endosomes on microtubules

Nature Cell Biology 1: 376 - 382

[Perisic 1999] Perisic, O. et al. (1999) Mapping the phospholipid-binding surface and translocation determinants of the C2 domain from cytosolic phospholipase A2. J. Biol Chem. 274: 14979-14987.

[Pfeffer 1995] Pfeffer, SR. et al. (1995) Rab GDP dissociation inhibitor: putting Rab GTPases in the right place. J. Biol. Chem. 270: 17057-17059.

[Rodman 2000] Rodman, JS. Wandering-Ness, A. (2000) Rab GTPases coordinate endocytosis. Journal Cell Science 113: 183-192

[Sackmann 1996] Sackmann, E. (1996) Thermo-elasticity and adhesion as regulators of cell membrane architecture and function, J. Phys. Condens. Matter 18: R785-R825

[Sackmann 2006] Sackmann, E., (2006) Thermo-elasticity and adhesion as regulators of cell membrane architecture and function. J. Phys.: Condens. Matter 18: R785-R825

[Sackmann 2010] Sackmann, E., Physics of Cellular Movements [2010] Annu. Rev. Condens. Matter Phys. 2010. 1:15.1-15.20

[Sackmann 2011] Sackmann, E. (2011) Quantal concept of T-cell activation: adhesion domains as immunological synapses

[Stahelin 2006] Stahelin, RV. et al. (2006) Structural and membrane binding analysis of the Phox homology domain of phosphoinositide 3-kinase-C2alpha. J Biol Chem. 281: 39396-39406.

[Vanhaesebroeck 2010] Vanhaesebroeck, B. et al. (2010) The emerging mechanisms of isoform-specific PI3K signalling Nature Rev. Mol. Cell Biol. 11: 329-341 (May 2010)

[Vergeres 1995] Vergères, G. (1995) The Myristoyl Moiety of Myristoylated Alanine-rich C Kinase Substrate (MARCKS) and MARCKS-related Protein Is Embedded in the Membrane J. Biol. Chem. 270: 19879-19887.

[Welti] Welti, R., et al. (2002) Profiling membrane lipids in plant stress responses. J. Biol. Chemistry 31: 994-32002, 2002.

[Werlem 1998] Werlen, G. et al. (1998) Calcineurin preferentially synergizes with PKC-theta to activate JNK and IL-2 promoter in T lymphocytes. EMBO J. 17: 3101-11.

[Whimbley 1996] Wimley, WC. , White S.H. (1996) Experimentally determined hydrophobic scale for proteins at membrane interfaces. Nat. Struct. Biol. 3: 842-848.

[Wu 1998] Wu, W., Nancollas, H. (1998) The understanding of the relationship between solubility and particle size. J. Solution Chemistry 27: 5201-5230

[YuAn 2003] Yu An (2003) Geranylgeranyl Switching Regulates Structure, 11: 347-357

[Zeng 1989] Zheng, Q., Gunton, (1989) Theory of Ostwald ripening for two-dimensional systems Phys Rev Letters 39: 4848-4852.

9.A.7 References to Appendix S.9. A

[Andelman 1995] Andelman, D. 1995. Electrostatic properties of membranes: the Poisson-Boltzmann theory. In Handbook of Biological Physics.

Elsevier Science, Amsterdam, The Netherlands.

[Andelman 1997] Diamant, H., Andelman, D. (1997) Adsorption kinetic of surfactants at fluid-fluid interfaces. Prog. Colloid Polym. Sci. 103:51-59.

[Haleva 2004] Haleva, E., et al (2004) Increased concentration of polyvalent phospholipids in the adsorption domain of a charged protein. Biophys. Journal 86: 2165-2178

[Harries 1998] Harries, D. et al. Structure, Stability, and Thermodynamics of Lamellar DNA-Lipid Complexes (1998) Biophys. J. 75: 159-173

[Jähnig 1990] Jähnig, F. (1980) Electrostatic free energy and shift of the phase transition for charged lipid membranes. Biophysical Chemistry 4: 309-318.

[Khelashvili 2008] Khelashvili, G., et al. (2008) Protein diffusion on charged membranes: A dynamic mean-field model describes time evolution and lipid reorganization Biophys J 94: 2580-2597

[Sackmann 1995] Sackmann, E. (1995) Physical basis of self-organization and function of membranes. Physics of Vesicles in 'Handbook of Biological Physics' Ch.V, (eds. R. Lipowsky und E. Sackmann Vol. Elsevier Amsterdam 1996.

